

Use of vertical electrical soundings to delineate seawater intrusion in a coastal area of Byunsan, Korea

Sung-Ho Song · Jin-Yong Lee · Namsik Park

Received: 29 August 2006 / Accepted: 9 October 2006 / Published online: 9 November 2006
© Springer-Verlag 2006

Abstract To delineate spatial extent of seawater intrusion in a small experimental watershed in the coastal area of Byunsan, Korea, electrical resistivity surveys with some evaluation core drillings and chemical analysis of groundwaters were conducted. The vertical electrical sounding (VES) method was applied, which is useful to identify variations in electrical characteristics of layered aquifers. The drilling logs identified a three-layered subsurface including reclamation soil, weathered layer and relatively fresh sedimentary bedrock. The upper two layers are the main water-bearing units in this area. A total of 30 electrical sounding curves corresponded mostly to the H type and they were further divided into three classes: highly conductive, intermediate, and low conductive, according to the observed resistivity values of the most conductive weathered layer. In addition, groundwater samples from 15 shallow monitoring wells were analyzed and thus grouped into two types based on HCO_3/Cl and Ca/Na molar ratios with TDS levels, which differentiated groundwaters affected by seawater intrusion from those not or less affected. According to relation-

ships between the three classes of the sounding curves and groundwater chemistry, locations of the monitoring wells with low HCO_3/Cl and Ca/Na ionic ratios coincided with the area showing the highly conductive type curve, while those with the high ratios corresponded to the area showing low conductive curve type. Both the low electrical resistivity and the low ionic ratios indicated effects of seawater intrusion. From this study, it was demonstrated that the VES would be useful to delineate seawater intrusion in coastal areas.

Keywords Seawater intrusion · Vertical electric sounding · Resistivity · Ionic ratio · Korea

Introduction

Seawater intrusion is one of the most common problems in coastal areas (Park et al. 2005; Lee and Song 2006; Sherif et al. 2006). Pollution of groundwater by seawater occurs when saline water displaces or mixes with freshwater in aquifers. One of the most common methods for assessing seawater intrusion through an aquifer in coastal areas is a periodic analysis of groundwater chemistry. When seawater intrusion is a main cause of high salinity, groundwater generally exhibits high concentrations not only in total dissolved solids (TDS) but also in major cations and anions (Richter and Kreitler 1993).

In a coastal aquifer, which is in contact with the sea, groundwater levels fluctuate in response to tidal variation (Todd 1980). In general with increase of distance from coastline, amplitudes of the fluctuation decrease and the time lag increases. To analyze the variations in groundwater level and its quality due to seawater

S.-H. Song (✉)
Rural Research Institute, Korea Rural Community
and Agriculture Corporation, Ansan 425-170, South Korea
e-mail: shsong84@hanmail.net; shsong@ekr.or.kr

J.-Y. Lee
GeoGreen21 Co., Ltd., 4th Floor, SEK Building,
1687-22, Bongchon6-dong, Gwanak-gu, Seoul 151-812,
South Korea

N. Park
Division of Civil and Ocean Engineering,
Dong-A University, 840 Hadan2-dong, Saha-gu,
Busan 604-714, South Korea

intrusion and tidal variation, periodic measurements of groundwater levels and analyses of groundwater quality are necessary, which requires installation of monitoring wells. However, appropriate placements of monitoring wells would be difficult without knowing the extent of seawater intrusion a priori.

To avoid excessive evaluation drillings to locate the seawater intrusion wedge, surface geophysics such as electrical resistivity surveys or electromagnetic methods may be used. Electrical resistivity surveys introduce electrical current into the ground by means of metal electrodes to detect the electrical conductivity (EC) of subsurface formation, which is an intrinsic property of the formation and the groundwater. Because the difference between the ECs of freshwater and seawater is significant, electrical resistivity surveys are well suited for studying the relationship between the two in coastal aquifers (Sherif et al. 2006). The VES, one-dimensional array method, is especially useful to reveal saline water zones and discontinuous layers because the signal to noise ratio of VES is higher than the two-dimensional array methods. However, VES may be subject to ambiguity problems because low resistivity may occur from various factors such as groundwater chemistry and formation materials (Zohdy et al. 1974). Thus, to delineate more reliably the zone of seawater intrusion, analysis of groundwater chemistry at available wells can be additionally conducted (Bear et al. 1999).

Meanwhile it was reported that more than 21% of shallow groundwaters within 10 km from the western coastline in Korea were affected by seawater intrusion (Park et al. 2002). This drew the attention of relevant governmental authorities (Ministry of Agriculture and Forestry, Korea Rural Community and Agriculture Corporation, Korea Water Resources Corporation, Korea Institute of Geoscience and Mineral Resources) and environmental communities (MOCT et al. 2005). To tackle these seawater intrusion problems in coastal areas and to devise appropriate technical measures, a variety of research projects and coastal groundwater monitoring programs have been undertaken in this country including this study.

The purpose of this study is to demonstrate potential applicability of electrical resistivity surveys, especially VESs to delineate the zone of seawater intrusion influence in an experimental watershed at the western coastal area of Byunsan, Korea. To further examine the analysis results of the VES at 30 points, chemical analyses of groundwaters from 15 newly installed shallow monitoring wells and some exploratory core drillings was conducted. In addition, to characterize hydrogeological properties of the coastal aquifer, consecutive monitoring data of groundwater level and

specific conductivity (SC) at two selected observation wells were also analyzed.

Materials and methods

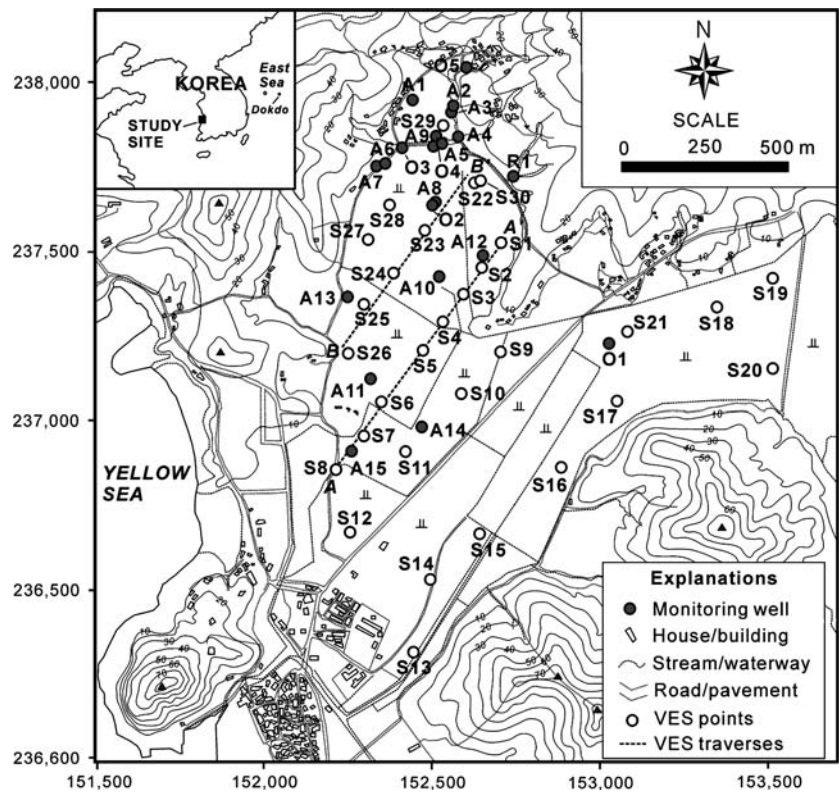
Hydrogeologic characteristics

The study area is in Byunsan-myon, Buan-gun, on the western coastal area of Byunsan peninsular, which is about 210 km from Seoul, capital of Korea (Fig. 1). The topography is generally flat in the central part where agricultural activities are concentrated. The flat area (0–3 m above sea level), about 4 km², is surrounded by a series of small mountains (40–50 m high above sea level). Average annual precipitation is 1,443 mm for the last 10 years (1996–2005) in this area, which is slightly larger than the mean for the whole country (1,260 mm) and over 60% of them occur in the summer season (Lee and Lee 2000). Average air temperature is 12.7°C and it is hottest in August and the lowest in December.

Most of the surrounding areas are paddy fields. Some residential houses are mainly distributed in the northern and southern parts of the study area. Most of the drinking water is supplied with serviced pipes. There exist some groundwater wells for agricultural or domestic use, which are situated 250–2,000 m away from the coast. Pumping at the wells mostly occurred in March–May for rice crops (Lee and Song 2006). Recently some of the wells experienced a large increase of groundwater salinity and thus were abandoned, which resulted in new installation of groundwater wells in more distant areas from the coast.

The hydrogeological sequence of the study area identified from data of well loggings and drilling cores is as follows: colluvial deposit or reclamation soil, a weathered zone, and bedrock (Fig. 2). Among these hydrostratigraphic units, the upper two are main water-bearing units. The colluvial deposits are distributed only at the bottom of small mountains with thickness ranges of 4–16 m but the reclamation soils widely occur in the central part of the study area, mostly paddy fields. Thickness of the reclamation layer ranged from 0.9 to 2.7 m and it is mostly comprised of silt and clayey silt. Below the reclamation layer, the weathered layer of the sedimentary rock is encountered. Thickness of this layer ranges between 2.3 and 15 m (actually not determined, see Fig. 2). Compositions of the weathered layer corresponded to sandy loam, loam, silty loam, or silty clay loam according to USDA textural classification (USDI 1974). The bedrock, considered less pervious, first occurs at depths of 7–18.3 m and it consists of a Cretaceous

Fig. 1 Location map of the study area showing the shallow groundwater monitoring wells. Coordinates along axis are TM in meter



sedimentary rock, which is extruded by volcanic rock. Interfaces among the layers are undulated and the thickness of each layer varies significantly with location.

Fifteen shallow wells (A1–A15) were newly installed for this study (see Fig. 1). Depth of the wells range between 0.93 and 16 m and the wells were screened into one of the three layers or both (Table 1). Results of pumping and slug tests conducted at these wells and some existing wells indicated that hydraulic conductivity of the reclamation layer ranged from 1.31×10^{-5} to 2.18×10^{-5} cm/s and that of the weathered layer ranged between 1.06×10^{-3} and 9.85×10^{-3} cm/s. The hydraulic conductivity of the upper portion of the bedrock is in the order of 10^{-5} cm/s. Values of the estimated hydraulic conductivity were not considered exactly representative of each layer because some of the wells were screened into the multiple layers.

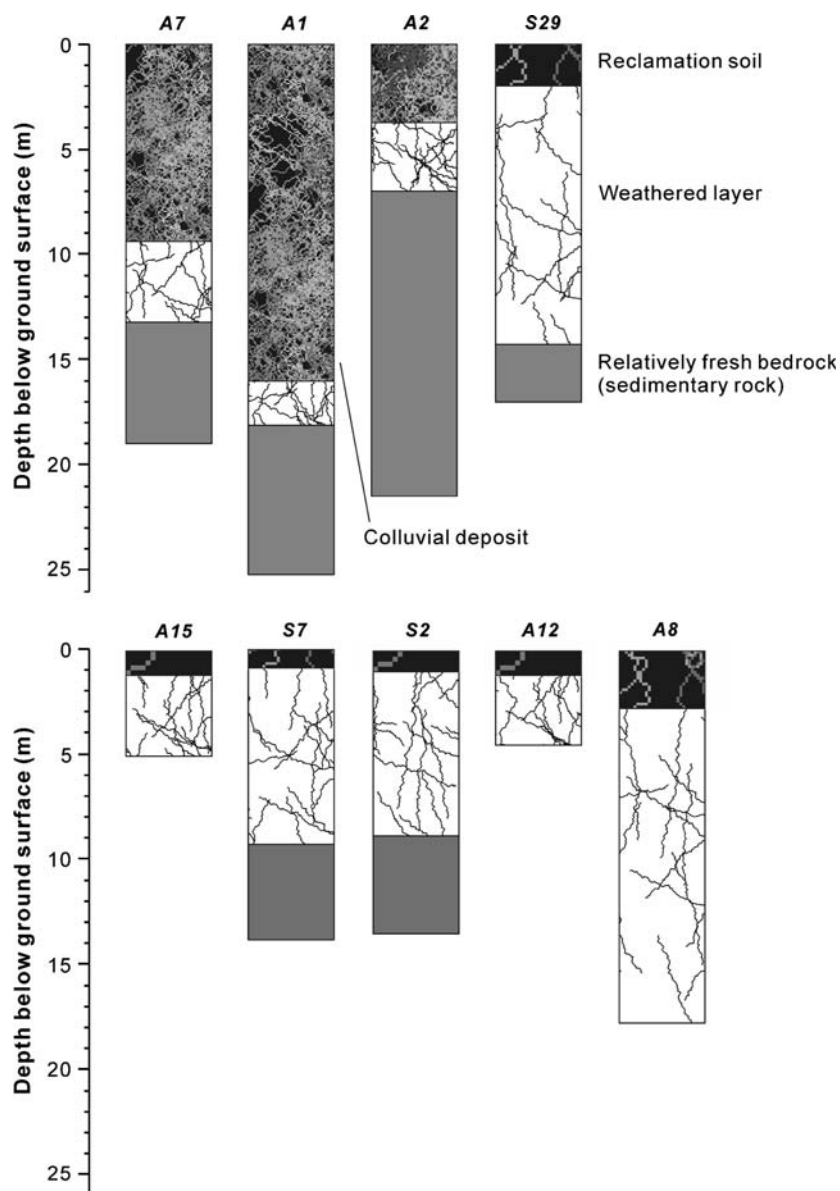
Water levels in the study area occurred at depths of 0.20–3.19 m below ground surface, which corresponded to –0.81 to 6.25 m above mean sea level. Except for single value (6.25 m for the uppermost well O5), they were between –0.81 and 1.86 m (mean = 0.42 m) above sea level. Relatively lower water levels in the upper part of the study area (convex water level contour) compared with those of the surrounding area are attributed to affect the topography and some groundwater pumping for domestic use. Annual fluctuation of the water levels was within 1 m except for a temporary

large decline during irrigation season but the water levels in this area were generally declining. Groundwaters generally flow from NE to SE direction towards the coast. Mean hydraulic gradient in the central area was 0.0087. It was steep at bottom of the hills while it became gentler towards the coastline.

Sinusoidal fluctuation of groundwater levels would occur in response to tides in coastal aquifers (Ataie-Ashtiani et al. 1999). Therefore, time series data such as groundwater level and SC with tidal variation can be analyzed in time domain. In this study, the fluctuations of groundwater levels were analyzed at O1 and O2 observation wells, which were drilled to about 60 m depth, during December of 2004. Figure 3a shows that the groundwater levels at the two wells fluctuated with similar pattern and were directly affected by precipitation on December 4, 2004. It was inferred that the aquifer characteristics are homogeneous as a whole because groundwater in the two observation wells responded nearly simultaneously to the site precipitation and because the fluctuation patterns of groundwater levels were nearly the same although the two observation wells are 700 m apart. Figure 3b shows that the variation patterns of SC and of groundwater level are nearly the same although a time lag existed.

Cross correlation was calculated to analyze the relation between tidal fluctuation and SC and water

Fig. 2 Simplified geologic sections at some selected locations



levels. The cross correlation, which is computed as a correlation between the input variable and output series, ranges between -1 and 1 (Yaffee and McGee 2000). Figure 4 shows that groundwater level is highly correlated with tide without any significant time lag and the SC also showed a good correlation with a time lag of 2 h. The peak coefficients of cross correlation are 0.3421 and 0.6766, respectively. These results indicated that the groundwater level and SC in the study area were strongly affected by the tidal variation.

Electrical resistivity surveys

The ability of a saturated subsurface formation to conduct electrical current depends primarily on three factors: porosity, connectivity of pores, and the SC of

the water in the pores (Telford et al. 1990). Pore water and its chemical character are especially dominant factors influencing the flow of the electric current because formation materials in general are resistant to electrical flow. An EC of a formation is also expressed as resistivity, the inverse of SC. Thus, resistivity decreases as porosity, hydraulic conductivity, and water salinity increase (Benkabbour et al. 2004).

To delineate the zone of seawater intrusion, VES surveys were performed at 30 points (see VES points in Fig. 1). Resistivity profiling was also constructed along two traverses to analyze the profile of seawater wedge (see traverses in Fig. 1). The lengths of electrodes were maintained constant at each point to avoid sparse data sampling. The electrode array method for VES was the Schlumberger array in which location of the potential

Table 1 Completions of the shallow monitoring wells in the study area

Well	X (m, TM)	Y (m, TM)	Elevation ^a (m, amsl)	Well depth (m)	Screen length ^b (m)	Water level ^c (m, amsl)
A1	152,441.92	237,947.98	2.77	16.0	6.0	1.67
A2	152,556.99	237,915.73	1.79	4.5	1.9	1.15
A3	152,561.72	237,930.19	2.21	7.5	2.3	1.51
A4	152,574.91	237,837.09	1.46	4.3	1.9	1.26
A5	152,523.50	237,815.02	1.75	6.6	1.7	0.80
A6	152,358.81	237,756.80	1.81	15.0	9.0	0.92
A7	152,334.01	237,751.57	3.03	10.5	4.5	1.74
A8	152,504.30	237,634.70	0.77	2.14	1.5	0.31
A9	152,509.50	237,806.10	0.87	1.5	1.5	0.60
A10	152,519.80	237,423.10	0.27	2.5	2.5	-0.78
A11	152,315.50	237,122.30	0.04	1.86	1.86	-0.60
A12	152,658.70	237,481.30	0.74	1.20	1.20	-0.36
A13	152,248.50	237,362.20	0.43	1.65	1.65	-0.58
A14	152,470.00	236,977.60	0.24	1.15	1.15	-0.53
A15	152,272.90	236,907.30	0.00	0.93	0.93	-0.48
O1	153,027.70	237,225.94	0.25	60.0	Open hole ^d	-0.81
O2	152,504.30	237,634.67	0.22	60.0	Open hole	-0.73
O3	152,408.85	237,805.37	1.68	60.0	Open hole	0.65
O4	152,530.92	237,826.06	1.50	80.0	Open hole	0.75
O5	152,603.33	238,044.46	7.08	80.0	Open hole	6.25
R1	152,740.35	237,722.79	5.04	96.0	Open hole	1.86

^a Surface elevation

^b Length of the screen from the well bottom

^c Measured on April 21, 2005

^d Left open except for upper casing of 2–3 m

Fig. 3 a Water level fluctuations in O1 and O2 observation wells with precipitation records during December of 2004. *Solid lines* indicate the amounts of precipitation. **b** Typical relationship between groundwater level and specific conductivity at O2 observation well

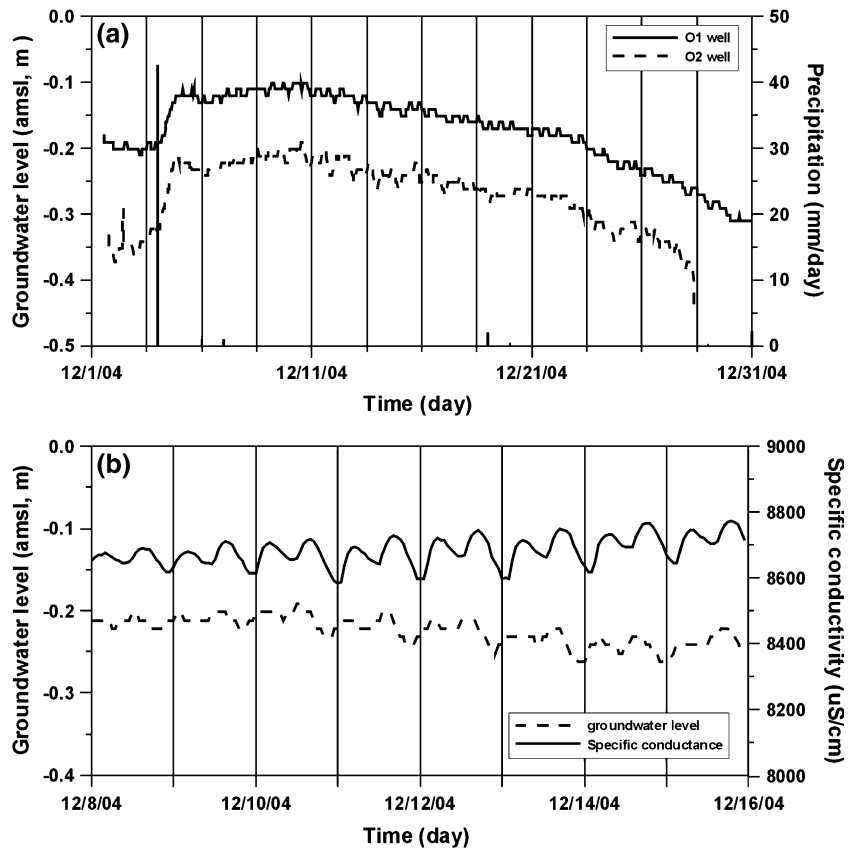
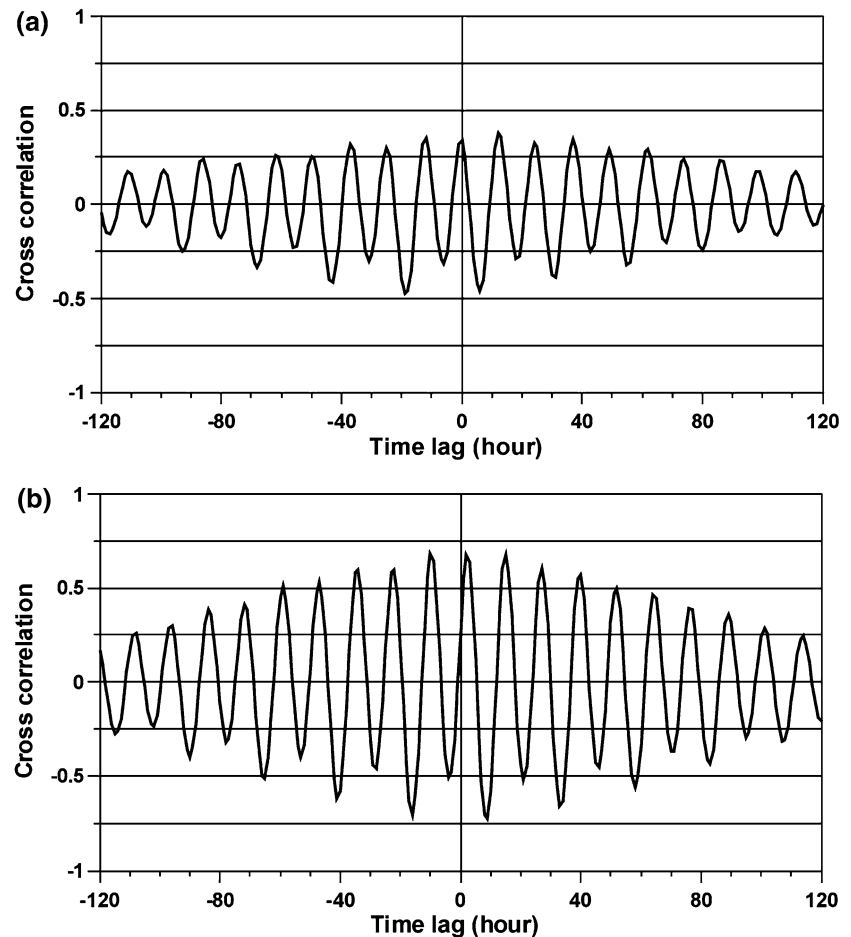


Fig. 4 Cross-correlations at O2 observation well between tide and (a) groundwater level and (b) specific conductivity



electrodes remained fixed while the current electrode spacing ($AB/2$) was symmetrically expanded from the center of the spread (Telford et al. 1990). Distances between neighboring sounding points ranged from 60 to 300 m.

Apparent resistivity is obtained from the ratio of the potential difference to the current, multiplied by the array constant. Therefore, apparent resistivity represents the structure of the EC in the multi-layered formation. Apparent resistivity curves for a three-layer structure generally fall into one of four typical types: K, H, A, and Q, determined from the vertical sequence of resistivity in each layer (Zohdy et al. 1974; Telford et al. 1990). Among them, the type H curve shows a relation with $\rho_1 > \rho_2 < \rho_3$, where ρ_1 , ρ_2 , and ρ_3 are the resistivity of the uppermost, intermediate and bottom layers, respectively. Resistivity at first decreases and later increases as $AB/2$ increases. This behavior implies that the middle layer is the best electrical conductor compared with the overlaying and underlying layers.

An inversion method of the damped least-squares technique was adopted for quantitative analysis of horizontal resistivity variation in each layer because

the problem of VES over a horizontally layered formation is nonlinear in the unknown parameters such as resistivity and thickness of each layer (Chyba 1986). A resistivity meter, STING R1 and electrode switch system, SWIFT (Advanced Geosciences, Inc.), were used for the resistivity data acquisition.

Chemical analysis of groundwaters

Groundwater samples were obtained from the 15 new monitoring wells in January and April 2005 (see the shallow wells in Fig. 1). Prior to sampling, water of at least three well volumes was purged and pH, EC and TDS were measured using standard field probes. Samples for cation analysis were filtered at 0.45 μm and preserved ($\text{pH} < 2$) using ultra pure HNO_3 in 125 ml HDPE bottles. Samples for anions were collected in 60 ml HDPE bottles through 0.45 μm filtration. Water samples of 125 ml were also collected for analysis of alkalinity. All samples were stored at 4°C in a cooler box until analysis. Anion constituents were analyzed by ion chromatography (IC, DX-120, DIONEX), and other cationic constituents were analyzed

by ICP-MS (Ultramass 700, Varian), AA (5100PC, Perkin Elmer) and ICP (ICP-IIIS, Shimadzu) following USEPA standard methods. Alkalinity was determined by potentiometric titration using Gran plots. It is generally expected that salinization of groundwater due to seawater intrusion is indicated by increases in TDS and major ions. Only major ions related to seawater intrusion are discussed in this study.

Results and discussion

Vertical electrical soundings

Simple interpretation of resistivity sounding data indicates that the shallow subsurface in the study area can be generally represented by two groups of three-layer geological models corresponding to the H (80%) and A (20%) type curves (Zohdy et al. 1974; Edet and Okereke 2001). Figure 5 shows observed apparent resistivity values versus depth ($AB/2$) and calculated layer thickness. The resistivity values initially decreased but they again increased after certain depths, which indicated the existence of a less resistive (more conductive) hydrogeologic layer between more resistive top and bottom layers.

Based on the three-layer model, average resistivity and thickness of each layer were computed (Table 2). The top layer showed resistivities of several tens ohm-m and it mostly corresponded to reclamation soil (silt and clayey silt) about 0.7–4.3 m thick. The middle layer is weathered rock layer and this is the major aquiferous unit in this area. The middle layer showed the lowest resistivities of 1–8 Ω -m and its thickness varies between 2.2 and 14.1 m except S11, S12 and S14 near the coastline. The anomalous high values of thickness in S11, S12 and S14 are supposed to be overestimated because input current is absorbed in the upper high conductive layer. Static water levels were generally in the bottom of the reclamation soil or in the top of the weathered layer (see Table 1). The saturated middle layer is the most conductive. The bottom layer of unresolved thickness is relatively fresh sedimentary rock and it has high resistivities over several hundreds ohm-m.

The sounding curves were further classified into three types: highly conductive, intermediately, and low conductive types depending on the relation of resistivities of the most conductive middle layer with those of the top and bottom layers. Sounding curves, which satisfy $\rho_3 \ll \rho_1$ and $\rho_2 < 5 \Omega$ -m, are called “highly conductive” type. Curves at S6, S7, S8, S10, S11, S12, and S14 belong to this type and these points are mostly

distributed near the coastline. Curves with $\rho_3 > \rho_1$ and $\rho_2 > 10 \Omega$ -m are called “low conductive” type, which included sounding locations of S1, S18, S19, S20, S22, S23, S24, S27, S28, S29, and S30. These points are relatively far from the coastline. The “intermediately conductive” type exhibiting a condition of $\rho_3 < \rho_1$ and $5 < \rho_2 < 10$, can be considered as transition characteristics between the highly conductive and low conductive types.

Two cross-sectional resistivity profiles were constructed along the traverses AA' and BB' (Fig. 6). These resistivity profiles show that the zone with resistivity lower than 5 Ω -m is distributed near the coast. This may be due to intrusion of the seawater from the coastline, and boundaries between low and high resistivities lower than 10 Ω -m formed between S1 and S6 and between S22 and S26, which are in the inland side of the traverses (see Fig. 1).

Spatial and vertical distribution of resistivity

To examine spatial distribution of resistivity values with depth, a kriging method was used. However, kriging generally smoothes out local details of the spatial variation of the attribute, with small values being overestimated and large values being underestimated (Cressie 1988). To construct a contour map without smoothing effects, a variogram analysis was conducted. Semivariogram (or traditionally variogram) analysis is a tool used to analyze how the data are spatially interconnected (Isaaks and Srivastava 1989) and semivariogram describes the variance distribution of the data given by relative location difference.

The semivariograms were calculated for the apparent resistivity values at each depth using the Gaussian model, which is generally combined with a small nugget effect to avoid numerical instabilities in interpolation algorithms and generation of artifacts in interpolated maps (Goovaerts 1997). The results of semivariogram analysis showed no significant differences in nugget and range but significant differences in sill with $AB/2$ variation (Table 3; Fig. 7). The small variations of nugget and range indicate that interconnection between pairs of apparent resistivities is quite high regardless of increase of $AB/2$. However, sill increases as $AB/2$ increases and it can be predicted that variance of apparent resistivities is greater at deep depth than at shallow depth.

Using the results of variogram analysis, apparent resistivity contour maps were constructed for depths of 5, 10, 15, and 20 m to examine the classification of the three curve types for delineating zone of seawater intrusion (Fig. 8). The area having apparent resistivity

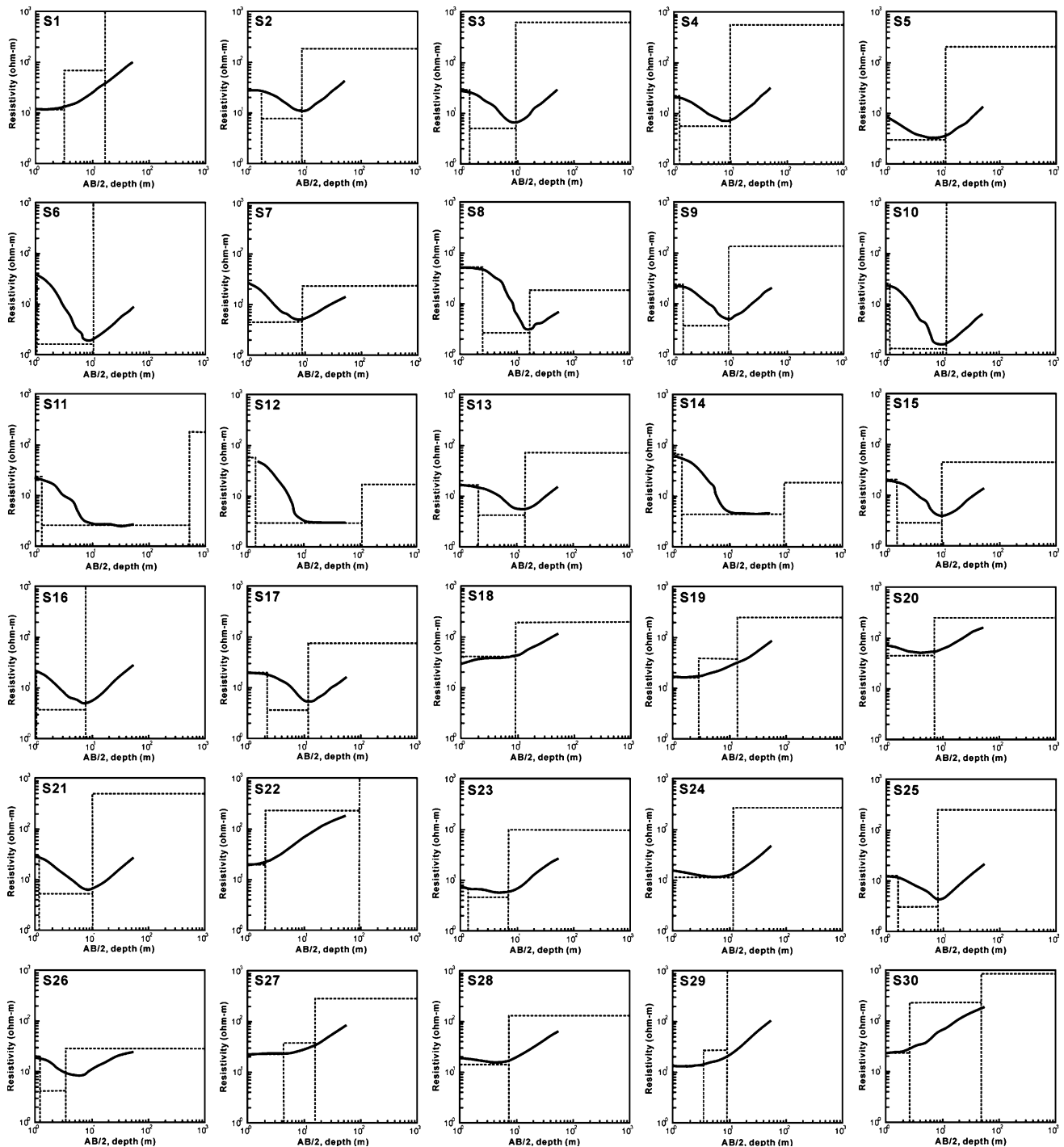


Fig. 5 Inversion results from VES with Schlumberger array at 30 points. *Box* indicates calculated layer thickness

lower than 5 Ω -m, which is considered as the effect of seawater intrusion, is mainly located in the southwestern part of the study area; and it is generally enlarged with depth, up to 15 m. However, this area is reduced at 20 m depth because there exist the less permeable sedimentary rocks at this depth (first

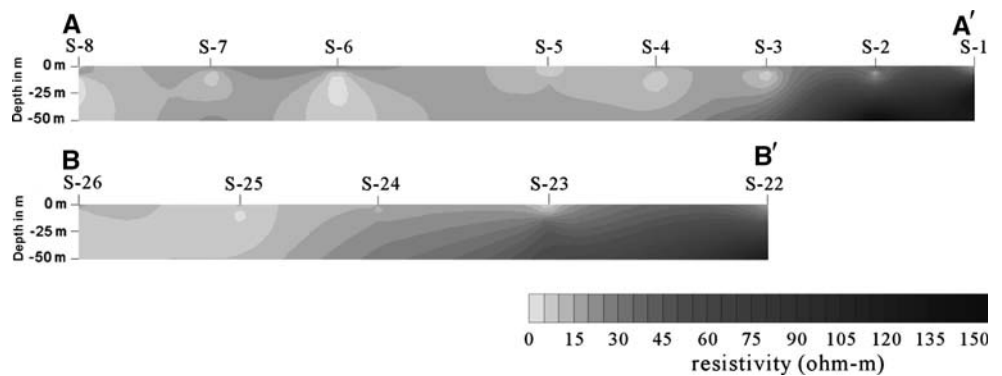
occurrence between 7.0 and 18.3 m). This observation is in accordance with the result of groundwater EC measurement. The SC values in shallow wells A10, A11, A13, A14, and A15, which are distributed in the southwestern part of the study area, are higher than 2,000 μ S/cm, equivalent to lower than 5 Ω -m. On the

Table 2 Inversion results of vertical electrical soundings

Location	VES curve type	Class of this study	Average layer resistivity (Ω -m)			Layer thickness (m)	
			ρ_1	ρ_2	ρ_3	t_1	t_2
S1	A	LC ^a	12	70	1,429	3.2	13.6
S2	H	I ^b	28	8	184	1.7	7.3
S3	H	I	29	5	610	1.4	8.0
S4	H	I	22	6	554	1.3	8.4
S5	H	I	10	3	202	0.8	10.4
S6	H	HC ^c	42	2	3,109	1.0	9.4
S7	H	HC	31	5	24	0.9	8.2
S8	H	HC	55	3	19	2.4	14.1
S9	H	I	25	4	137	1.4	7.9
S10	H	HC	26	1	1,162	1.2	10.3
S11	H	HC	24	3	181	1.3	529.3
S12	H	HC	57	3	17	1.4	102.6
S13	H	I	17	4	73	2.0	11.5
S14	H	HC	65	4	18	1.4	87.5
S15	H	I	21	3	46	1.5	8.0
S16	H	I	23	4	2,924	1.0	6.6
S17	H	I	21	4	77	2.2	9.3
S18	A	LC	1	41	199	0.1	9.2
S19	A	LC	17	39	252	2.8	10.7
S20	H	LC	82	45	250	0.7	6.4
S21	H	I	32	5	500	1.1	9.1
S22	A	LC	20	233	1,772	2.0	90.3
S23	H	LC	7	5	98	1.3	5.6
S24	H	LC	16	11	265	0.7	10.5
S25	H	I	12	3	245	1.6	6.4
S26	H	I	20	4	29	1.2	2.2
S27	A	LC	23	37	287	4.3	11.1
S28	H	LC	19	14	132	1.0	6.0
S29	A	LC	14	28	986	3.4	5.4
S30	A	LC	24	235	853	2.6	45.9

^a LC low conductive
^b I intermediately conductive
^c HC highly conductive

Fig. 6 Resistivity profiles showing the low resistivity zones due to the intrusion of seawater wedge. *S* indicated the location of VES points and *dots* represent the spacing of current electrodes (AB/2)



other hand, the SC for more inland wells are less than 1,000 μ S/cm and resistivities at their vicinities are higher than 10 Ω -m.

Table 3 Parameters of the variogram analysis for the Gaussian model

Depth (m)	Nugget	Sill	Range	r^2
5	0.1	81.93	141	0.939
10	0.1	278.5	165	0.807
15	1	506.9	167	0.776
20	1	793	168	0.769

Figure 9 shows the columnar sections with calculated resistivities representing each curve type and nearby soil profiles with estimated resistivities from EC measurement for soils. The resistivity profile at S7 belonging to the highly conductive type and the resistivity of middle layer of 5 Ω -m, indicated the influence of seawater intrusion (Fig. 9a). This result is in accordance with that of chemical analysis for soil samples that the SC of soil at A15, in the close proximity to S7, is 1.3 Ω -m. The resistivity of S2 representing the intermediately conductive type may be considered as

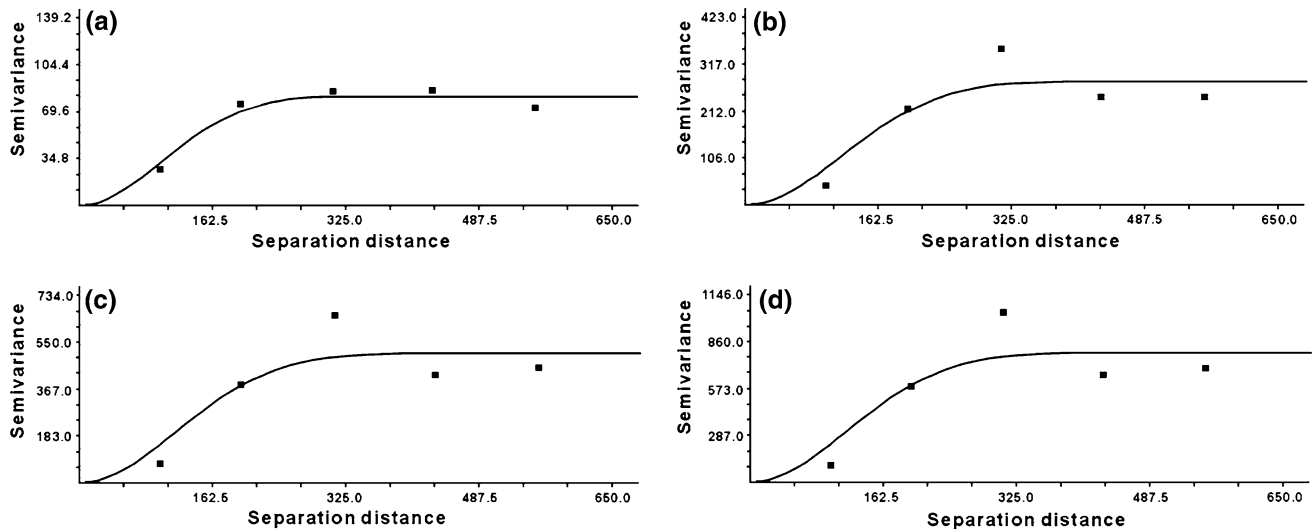


Fig. 7 Semivariograms for the Gaussian model at each depth. **a** 5 m, **b** 10 m, **c** 15 m, and **d** 20 m

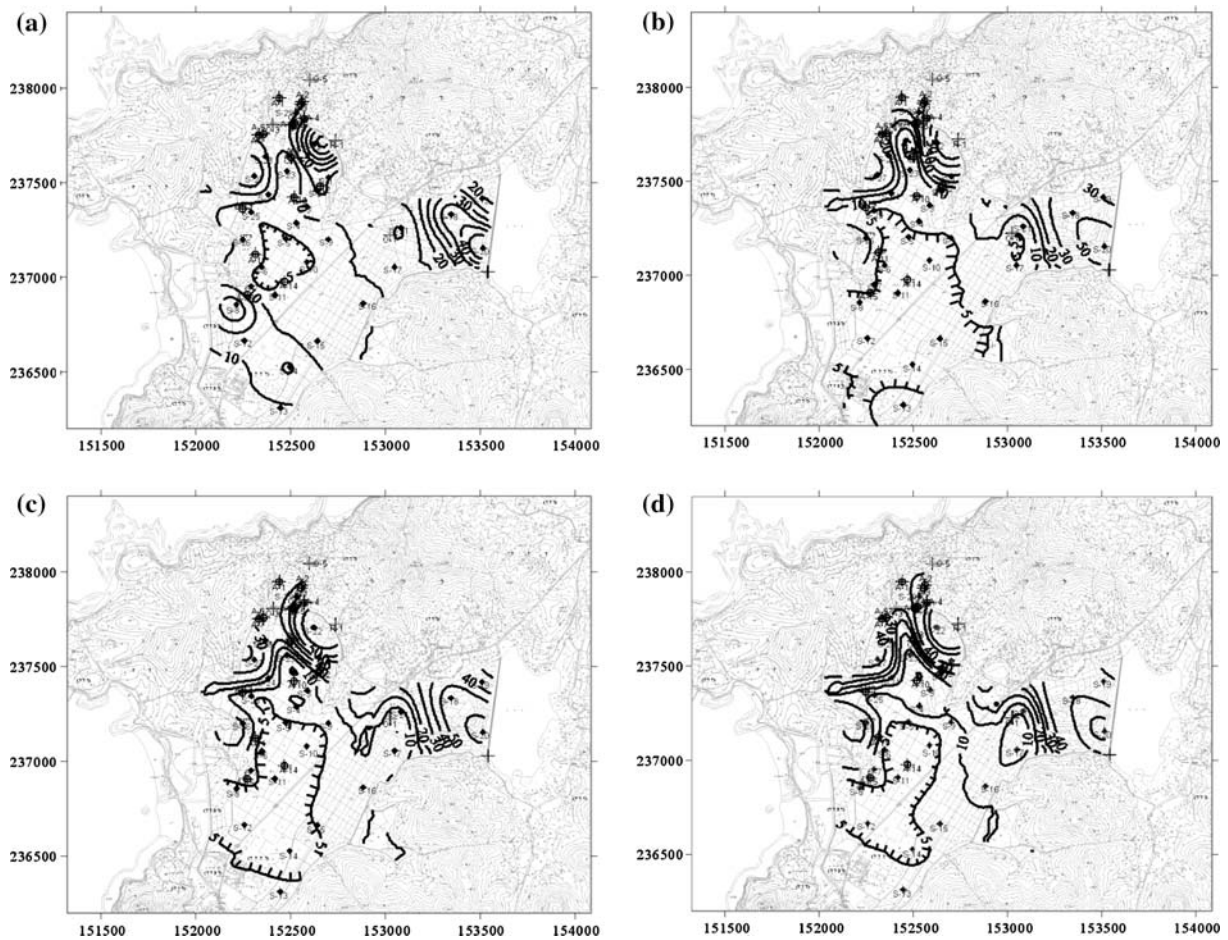


Fig. 8 Apparent resistivity contour map for depth of **a** 5 m, **b** 10 m, **c** 15 m, and **d** 20 m showing the extent of seawater intrusion region (hatched region below 5 Ω -m). Closed circles and diamonds indicate the shallow wells and VES points, respectively

transition characteristics from highly conductive to low conductive (Fig. 9b). The resistivity profile at S29 belongs to the low conductive type. At that point, high resistivities of several hundreds of ohm-m implied that this location was not affected by seawater intrusion (Fig. 9c). Estimated resistivity of the soil sample at A8, near S29, is 10.4 Ω-m. Consequently, the inversion results of VES data are generally well consistent with the EC measurements of the soil columns.

Groundwater chemistry

Results of the chemical analysis are given in Table 4. The pHs of the groundwater were least varying and they were near neutral (6.3–7.5). TDS was very much varying between 327 and 6,946 mg/l and it was closely correlated with EC (slope = 0.64, $r^2 = 0.995$). The EC of groundwater varied from 456 to 11,590 μS/cm, equivalent to the resistivity ranges of 0.9–21.9 Ω-m, indicating that the shallow aquifer is generally highly conductive. In the mean while, EC values of groundwater greater than 2,000 μS/cm require a mitigation measure in the country.

Sodium and chloride are the dominant ions of seawater, while calcium and bicarbonate are generally the major ions of fresh water (Hem 1989). Thus high levels of Na and Cl ions in coastal groundwater may indicate significant effect of seawater mixing, while the considerable amounts of HCO₃ and Ca mainly reflect the contribution from water–rock interaction (Park et al. 2005). The plot of HCO₃/Cl versus TDS shows that the regression slope is negative in the high (>2,000 mg/l) TDS concentration range, while the slope is positive in the low (<1,000 mg/l) TDS concentration range (Fig. 10a). This result may indicate that groundwater with high TDS concentrations is enriched with chloride due to seawater intrusion, and that groundwater with low TDS concentrations is not or less affected by seawater. Variation of Ca/Na ratio with TDS shows a similar trend and subsequently similar interpretation (Fig. 10b).

The resistivity values of groundwater samples with high TDS concentrations vary from 0.9 to 3.0 Ω-m, which is slightly higher than the average resistivity of seawater, 0.2 Ω-m (Telford et al. 1990). Therefore, the groundwater samples can be classified into two groups based on the TDS levels and the ionic ratio: one group of groundwater is under the influence of seawater intrusion and the other is not or less affected by the seawater. The former group is in the proximity to the coast and the latter one is distributed at the bottom of the small mountains (residential area). This classification can also be reconfirmed by a bivariate plot of Cl and NO₃ concentrations, in which, two groups were also extracted (Fig. 11). The two parameters generally represent effects of seawater intrusion and anthropogenic origin such as septic tank leakage or chemical fertilizers, respectively, in coastal aquifers (Kim et al. 2003). Consequently, areal distribution of the affected groundwater by seawater intrusion inferred from the groundwater chemistry data is quite similar to that determined by VES data.

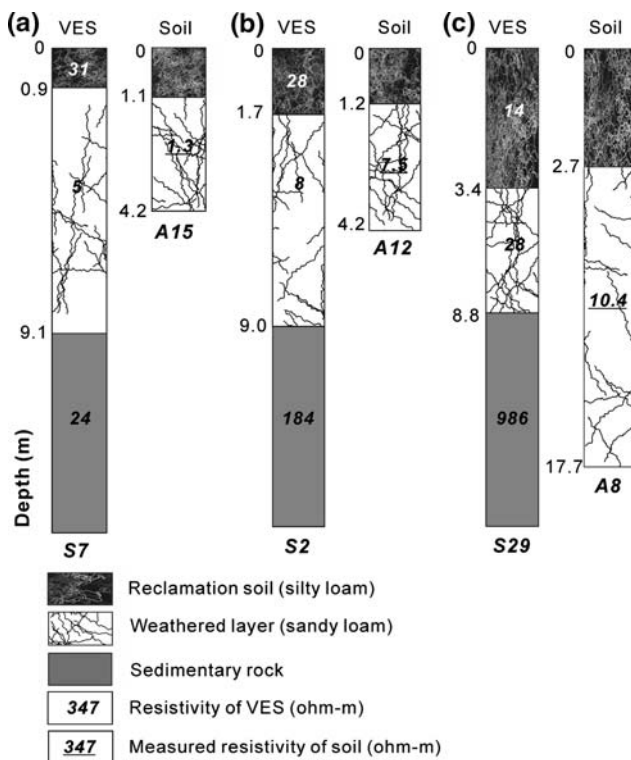


Fig. 9 Comparison of resistivities between calculated at VES points and measured in soils at three categories. *S* and *A* represent VES points and sampling points, respectively. **a** Highly conductive, **b** intermediately, and **c** low conductive types

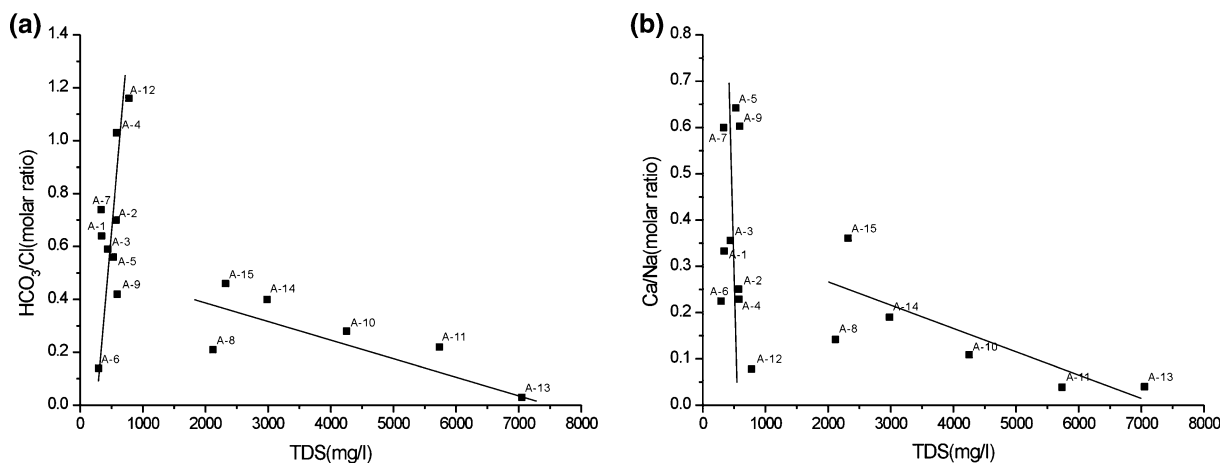
Conclusions

VESs were conducted to delineate seawater intrusion in a western coastal area of Korea. The resultant sounding curves mostly corresponded to the H type in which the resistivity decreased at first and then increased from certain depths. These results indicated the existence of the highly conductive layer between the upper and bottom layers, which was confirmed by the drill logging data. The most conductive middle layer was identified as water-bearing weathered rock layer. Based on the resistivity of the middle layer and

Table 4 Analysis results of the shallow groundwater samples in the coastal area of, Byunsan, Korea

Sample number	pH (SU)	TDS (mg/l)	EC ($\mu\text{S}/\text{cm}$)	Unit: mg/l							
				Na	K	Ca	Mg	Cl	HCO ₃	SO ₄	NO ₃
A1	6.7	337	456	46.48	3.74	26.98	7.93	63.67	70.15	17.00	72.42
A2	7.2	565	812	98.65	13.47	43.16	15.34	127.04	152.50	71.17	21.60
A3	6.9	434	619	56.17	5.95	34.90	18.05	72.32	73.20	38.93	105.92
A4	7.1	572	771	91.61	12.69	36.56	19.33	94.69	167.75	58.33	62.93
A5	7.2	521	732	67.03	2.43	75.07	5.58	123.04	118.95	76.37	13.86
A6	6.3	290	459	45.44	2.97	17.81	12.04	78.30	18.30	6.57	80.67
A7	7.2	329	480	35.02	4.13	36.62	18.47	53.07	67.10	36.22	65.46
A8	6.9	2,090	3,340	464.36	53.05	114.84	102.45	807.50	289.75	233.20	0.00
A9	7.0	581	848	79.79	5.34	83.89	18.79	152.30	109.80	105.70	0.00
A10	7.5	4,196	6,010	1,011.75	102.05	191.47	192.52	1,487.20	719.80	470.40	0.00
A11	7.9	5,658	8,310	1,737.51	103.71	118.75	187.83	2,207.00	829.60	445.70	0.00
A12	7.5	767	999	164.76	19.20	22.28	18.56	148.50	295.85	55.70	20.20
A13	7.2	6,946	11,590	2,003.64	117.73	138.07	298.81	3,541.40	207.40	624.20	0.00
A14	7.4	2,941	4,180	627.11	57.57	207.21	107.38	983.80	677.10	263.00	0.00
A15	7.4	2,289	3,320	393.64	43.12	247.60	75.22	710.60	558.15	244.20	0.00
Max	7.9	6,946	11,590	2,003.64	117.73	247.60	298.81	3,541.40	829.60	624.20	105.92
Min	6.3	290	456	35.02	2.43	17.81	5.58	53.07	18.30	6.57	0.00
Mean	7.2	1,901	2,862	461.53	36.48	93.01	73.22	710.03	290.36	183.11	29.54
Median	7.2	581	848	98.65	13.47	75.07	18.79	148.50	167.75	76.37	13.86
SD ^a	0.4	2142	3,390	637.55	41.30	74.38	89.09	1,010.33	269.78	193.01	37.03

^a *SD* standard deviation

**Fig. 10** Molar ratios of **a** HCO₃/Cl and TDS concentration and **b** Ca/Na and TDS concentration

its relation with those of the top and bottom layers, the sounding curves were further divided into three classes including highly, intermediately and low conductive. The highly conductive zone was mainly distributed in near coastal area, which indicated substantial influence of seawater intrusion.

Estimation of the seawater intrusion zone by VES was evaluated using groundwater chemistry data. Representative ionic ratios, HCO₃/Cl and Ca/Na, and TDS levels differentiated groundwater strongly

affected by the seawater intrusion from those not or less affected. Locations of the monitoring wells with the low ionic ratios and the high TDS levels matched well those of the low resistivity area determined by VES. In addition, resistivity contour maps with depth constructed by using a variogram analysis and three columnar sections of calculated resistivities compared with measured soil samples appeared very useful to delineate spatial and vertical distribution of seawater influence.

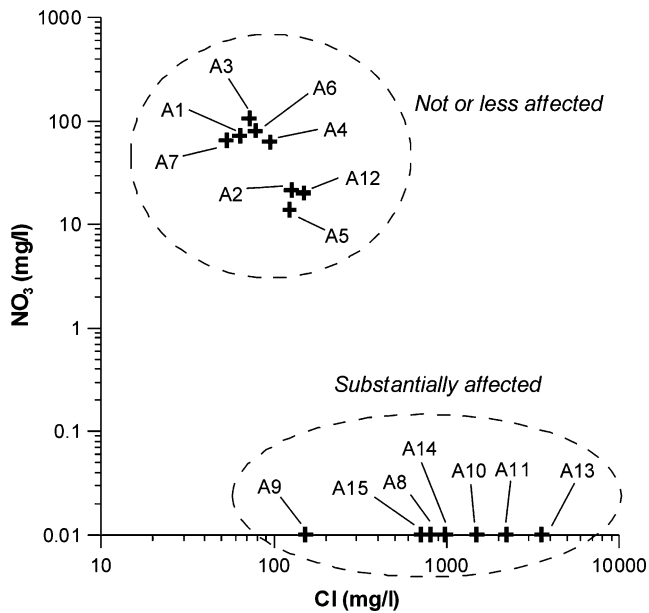


Fig. 11 Plot of Cl versus NO₃ concentrations. NO₃ concentration of 0.00 in Table 4 was regarded as the detection limit (0.01 mg/l) for the logarithmic plot

Acknowledgments This research was supported by a grant (code number 3-3-2) from Sustainable Water Resources Research Center of 21st Century Frontier Research Program.

References

Ataie-Ashtiani B, Volker RE, Lockington DA (1999) Tidal effects on sea water intrusion in unconfined aquifers. *J Hydrol* 216:17–31

Bear J, Ouazar D, Sorek S, Cheng A, Herrera I (1999) Seawater intrusion in coastal aquifers. Springer, Berlin Heidelberg New York, p 640

Benkabbour B, Toto EA, Fakir Y (2004) Using DC resistivity method to characterize the geometry and the salinity of the Plioquaternary consolidated coastal aquifer of the Mamora plain, Morocco. *Environ Geol* 45:518–526

Chyba J (1986) Some improvements in the interpretation of vertical electrical sounding curves. *Geophys Prospect* 34(6):913–922

Cressie N (1988) Spatial prediction and ordinary kriging. *Math Geol* 20(4):405–421

Edet AE, Okereke CS (2001) A regional study of saltwater intrusion in southeastern Nigeria based on the analysis of

geoelectrical and hydrochemical data. *Environ Geol* 40:1278–1289

Goovaerts P (1997) Geostatistics for natural resources evaluation. Oxford University Press, New York

Hem JD (1989) Study and interpretation of the chemical characteristics of natural water. U.S.G.S. Water-Supply Paper, vol 2254, US Government Printing Office, Washington DC

Isaaks EH, Srivastava RM (1989) Applied geostatistics. Oxford University Press, New York

Kim JH, Kim RH, Lee J, Chang HW (2003) Hydrogeochemical characterization of major factors affecting the quality of shallow groundwater in the coastal area at Kimje in South Korea. *Environ Geol* 44:478–489

Lee JY, Lee KK (2000) Use of hydrologic time series data for identification of recharge mechanism in a fractured bedrock aquifer system. *J Hydrol* 229:190–201

Lee JY, Song SH (2006) Evaluation of groundwater quality in coastal areas: implications for sustainable agriculture. *Environ Geol* (accepted)

MOCT (Ministry of Construction and Transportation), KOW-ACO (Korea Water Resources Corporation), KIGAM (Korea Institute of Geoscience and Mineral Resources) (2005) Research report on measures for potential groundwater hazard areas. KIGAM, Daejeon, p 579

Park SC, Yun ST, Chae GT, Lee SK (2002) Hydrogeochemistry of shallow groundwaters in western coastal area of Korea: a study on seawater mixing in coastal aquifers. *J Kor Soc Soil Groundw Environ* 7:63–77

Park SC, Yun ST, Chae GT, Yoo IS, Shin KS, Heo CH, Lee SK (2005) Regional hydrochemical study on salinization of coastal aquifers, western coastal area of South Korea. *J Hydrol* 313:182–194

Richter BC, Kreitler CW (1993) Geochemical techniques for identifying sources of ground-water salinization. CRC Press, p 258

Sherif M, El Mahmoudi A, Garamoon H, Kacimov A, Akram S, Ebraheem A, Shetty A (2006) Geoelectrical and hydrogeochemical studies for delineating seawater intrusion in the outlet of Wadi Ham, UAE. *Environ Geol* 49:536–551

Telford WM, Geldart LP, Sheriff RE (1990) Applied geophysics, 2nd edn. Cambridge University Press, New York

Todd DK (1980) Groundwater hydrology, 2nd edn. Wiley, New York

USDI (US Department of the Interior) (1974) Earth manual, a water resources technical publication, 2nd edn. US Government Printing Office, Washington DC, pp 14–17

Yaffee R, McGee M (2000) Introduction to time series analysis and forecasting. Academic

Zohdy AAR, Eaton GP, Mabey DR (1974) Application of surface geophysics to ground-water investigation. Techniques of water-resources investigations of the United States Geological Survey, book 2, chap D1, p 66